Connective Tissue Research, 44(Suppl. 1): 184–188, 2003

0300-8207/03 $12.00 + .00
DOI: 10.1080/03008200390152304

Taylor&Francis
healthsciences

Proteoglycans in Predentin: The Last 15 Micrometers Before Mineralization

M. Goldberg,[1] O. Rapoport,[1] D. Septier,[1] K. Palmier,[1] R. Hall,[2] G. Embery,[2] M. Young,[3] and L. Ameye[3]

[1]*Faculté de Chirurgie Dentaire, Université Paris, France*
[2]*Clinical Dental Science, Liverpool Dental School, University of Liverpool, United Kingdom*
[3]*Craniofacial and Skeletal Diseases Branch, NIH, Bethesda, Maryland, USA*

Small leucine-rich proteoglycans (SLRPs) regulate extracellular matrix organization. In order to investigate the distribution and potential functions of decorin, biglycan (BGN), and fibromodulin (3 SLRPs, potentially related to dentinogenesis), we performed light and electron immunochemistry on teeth from rats, and on wild-type and biglycan knockout mice (BGN KO). Immunohistochemical data demonstrate that chondroitin sulfate/dermatan sulfate (CS/DS) and keratan sulfate (KS) distributions displayed reverse gradients in predentin. The decrease of CS/DS labeling from the proximal to the distal predentin contrasted with the sharp decorin increase observed in the distal predentin near the predentin/dentin transition, an effect possibly attributable to the deglycosylation action of stromelysin-1. In contrast, BGN concentration was apparently constant throughout the whole predentin. Additional immunolabelings showed, for the first time, the presence of fibromodulin in predentin. Compared with the wild-type mouse, the mean diameter of collagen fibrils in the BGN KO was smaller in the proximal predentin but larger in the central and distal predentin, the metadentin was broader, and the dentin mineralization appeared altered and heterogeneous. Altogether, our data suggest an important role for BGN in dentin formation and mineralization.

Keywords Biglycan, Decorin, Dentin, Fibromodulin, Mineralization, Proteoglycans.

INTRODUCTION

Biochemical analyses have established that glycosaminoglycans (GAGs), covalently attached to a protein core as proteoglycans (PGs), are critical components of the predentin and dentin extracellular matrix. Histochemical and radioautographic investigations also demonstrate that the distribution of GAGs and PGs in dentin and predentin is different, showing a highly controlled temporal and spatial pattern of expression, implying that GAGs and PGs may have some functional implications in dentinogenesis [for review, 1–3]. We have previously shown that two distinct groups of sulfated GAGs are secreted by odontoblasts. The first group is secreted together with collagen fibrils in the proximal predentin, near the odontoblast cell bodies, whereas the second group is secreted distally, at the border where dentin undergoes mineralization [4]. CS/DS and KS-containing GAGs have been immunolocalized in dentin [5, 6]. These GAGs are present in small leucine-rich proteoglycans (SLRP) [7, 8]. Five SLRPs (decorin, biglycan, fibromodulin, lumican, and osteoadherin/osteomodulin) are known to be components of the predentin and dentin matrix [2, 3, 6, 9–12]. Decorin (DCN) and biglycan (BGN) are two CS/DS SLRPs, while fibromodulin (FM), lumican (LM), and osteoadherin/osteomodulin are primarily substituted with KS chains. Although SLRPs are present in predentin and dentin matrices, their role in dentinogenesis needs further clarification.

In predentin, gradients of GAG distribution that may have some functional implications have been visualized [5, 6]. There, DCN and BGN are thought to be involved in collagen assembly from the proximal area, where nascent collagen fibrils are secreted to the distal area and where before being mineralized, mature collagen fibrils are incorporated into dentin (13). Conflicting views have been expressed on the role of SLRPs in the initial mineral formation. PGs have been considered either as nucleators of mineralization, acting as a cation-exchanging calcium reservoir, or as inhibitors. The conclusions of these experiments strongly depended on the biological or in vitro models that were used and also whether the experiments were carried out in aqueous solutions, in gels, on a solid surface [14–18].

Therefore, there is still a need for mapping the distribution of PGs throughout predentin and in dentin. Light and electron immunohistochemistry provide useful tools for visualizing SLRPs and for studying their concentrations in situ. To gain insight

Received 9 November 2001; accepted 2 March 2002.
Address correspondence to Michel Goldberg, Faculté de Chirurgie Dentaire, Université Paris V, 1, rue Maurice Arnoux, 92120 Montrouge, France. E-mail: mgoldod@aol.com

TABLE 1
Observations with light microscope immunostaining in the mouse first molar at day 1.

	Pulp	Od	Predentin	Dentin	Presecretory and secretory ameloblasts	Enamel organ
Decorin	+	+	++++	± DEJ underlined	++	Junction ameloblasts/SI +++
Biglycan	++	++	++++	±	++	Junction ameloblasts/SI ++++ (SI +++)
Fibromodulin	±	±	++	−	Distal end only: ++	SI ++

Od = odontoblasts, DEJ = dentino-enamel junction , SI = stratum intermedium.

into the potential function that these molecules play during the formation and mineralization of dental tissues, we report here SLRP immunolabelings of predentin and dentin along with observations made on BGN KO mice.

MATERIALS AND METHODS

Light and Electron Microscopic Immunolabelling of Rat Incisors

The forming part of mandibular incisors of Sprague–Dawley male rats (100 g body weight) was used for immunohistochemical visualization of GAGs and PGs. Investigations were carried out on the predentin and dentin of undemineralized rat incisors, fixed with paraformaldehyde and processed for conventional light microscopy. The nature of the molecules in the forming part of the incisors, and the specificity of the antibodies that were used, were confirmed by Western blotting. The immunostaining was carried out with primary antibodies raised against anti-DCN (LF-113), anti-BGN (LF-107), and anti-FM (LF-150) (generous gift from Dr Larry Fisher, CSDB, NIDCR, NIH, Bethesda, MD, USA) [19]. This was followed by incubation with the secondary antibody, a peroxidase-conjugated goat antimouse IgG (Dako A/S, Denmark). The immunoreactivity was detected with diaminobenzidine diluted with PBS. Controls were carried out by adsorption, using the antibody with the protein at appropriate concentrations, and also by omitting the primary antibody.

After intracardiac perfusion of a glutaraldehyde/paraformaldehyde fixative, and low-temperature embedding in Lowicryl, ultrathin sections were labeled with colloidal gold/antibody complexes (10 nm diameter colloidal gold, Sigma Chemical, St. Louis, MO, USA). The sections were stained with uranyl acetate and lead citrate and examined with a Jeol 100B transmission electron microscope operating at 80 kV. On micrographs enlarged to a final magnification of 54000, gold particles were scored in 400 mm^2 square areas (2×2 cm) in the proximal, central, and distal predentin divided into three equal parts, and in metadentin [20]. Results were expressed in square micrometer of matrix.

Generation and Genotyping of BGN Knockout Mice

All experiments were performed under an institutionally approved protocol for the use of animals in research (#NIDCR-IRP-98-058 and 01-151). Mice deficient in BGN were generated by gene targeting in embryonic STEM cells [21]. All mice were genotyped by PCR analysis using DNA isolated from a small tail biopsy as described by Chen et al. [22]. PCR products were resolved by electrophoresis through 1.8% agarose gels yelding bands that were 212 bp for wt BGN allele and 310 bp for targeted BGN allele.

Light Immunohistochemistry and Electron Microscopy of KO Mice

BGN KO mice were killed 1 day after birth by decapitation with a razor blade, and mandibles were immersed in the fixative solution. Mandibles were processed for light and electron microscopy as reported above. Tissues from wild-type mice were processed simultaneously as controls. Undermineralized sections of paraplast-embedded mouse mandibles were dewaxed and immunostained with anti-DCN, anti-BGN, and anti-FM antibodies. Ultra-thin sections of Epon-embedded newborn mouse containing molars and incisors were stained with uranyl acetate and lead citrate and examined with a Jeol 100B transmission electron microscope operating at 80 kV. Micrographs enlarged at a final magnification of 54000 were used for direct measurement of collagen fibril diameter in the inner, central, and distal thirds of predentin (about 5 μm each).

RESULTS AND DISCUSSION

Immunolabeling of GAGs and PGs

We have previously reported that immunostaining with 2B6, an anti-CS/DS antibody, reveals a decreasing gradient from the

TABLE 2
Mean value (followed by the standard error) of the diameter of collagen fibrils in the proximal, central, and distal thirds of the predentin of wild-type and BGN KO mice.

	Wild-type		BGN KO	
Proximal predentin	16,3 ± 1,0 nm	**a**	7,9 ± 0,3	**a'** *
Central predentin	34,0 ± 0,7 nm	**b**	47,3 ± 0,7 nm	**b'** *
Distal predentin	36,1 ± 0,9 nm	**c**	51,6 ± 1,1 nm	**c'** **

* **a** vs. **a'** and **b** vs. **b'**: $p \leq 0.01$.
** c vs. **c'**: $p \leq 0.001$.
The difference between **a** vs. **c** is statistically significant ($p \leq 0.001$); but the difference between **b** and **c** is statistically nonsignificant.

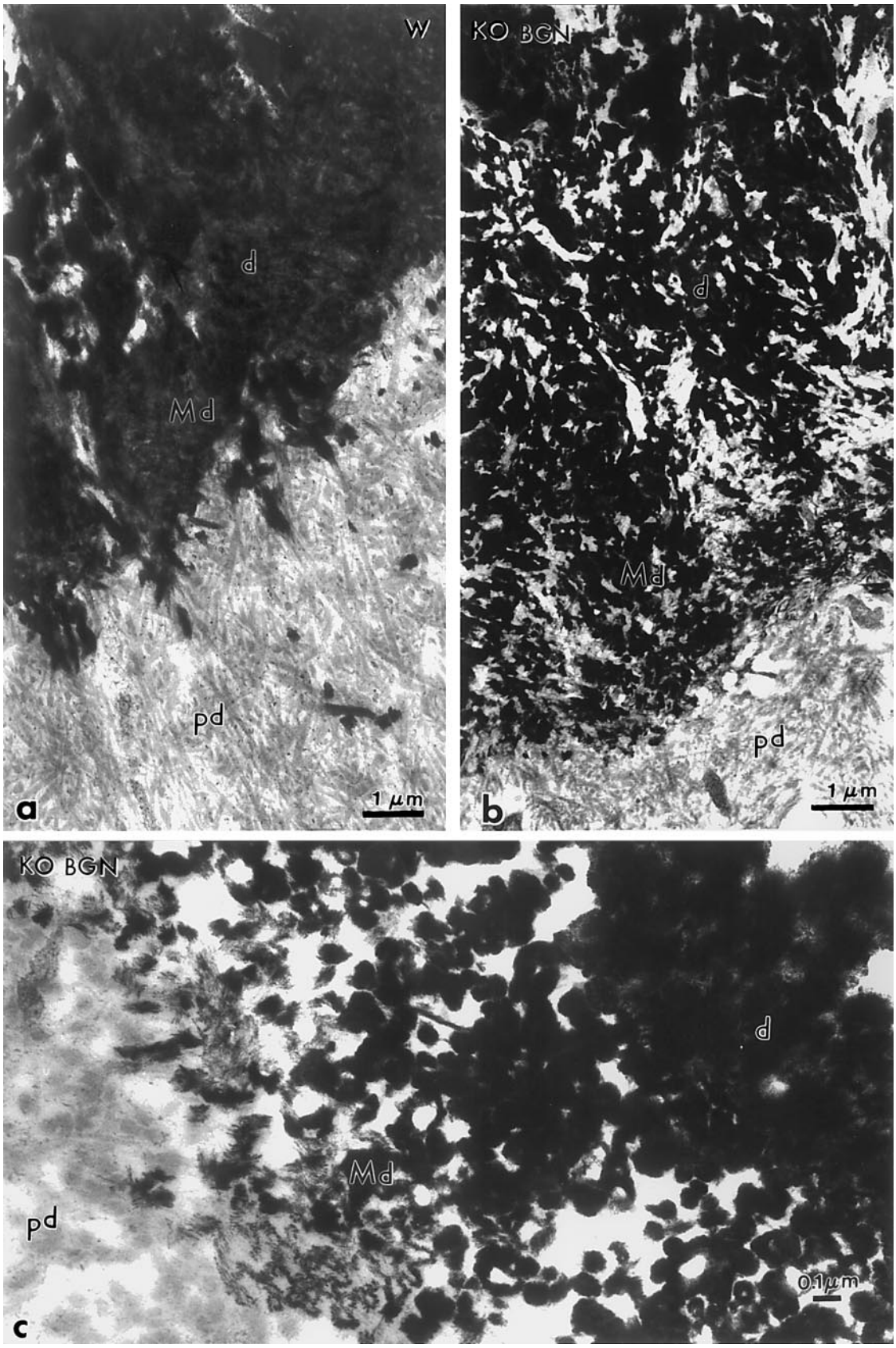

Figure 1. (a) In a wild-type (W) mouse molar, appearance of predentin (pd), metadentin (Md), and dentin (d) (×12,500). (b) In the BGN KO, in the mouse molar predentin (pd), the spatial organization of collagen fibril is altered. Metadentin (Md) is porous, and dentin (d) has an heterogeneous appearance (×10,800). (c) In the BGN KO mouse, metadentin is larger than in the wild-type mouse, especially porous and hypomineralized. Dentin is formed by calcospherites, separated by thin and larger interglobular spaces (×54,000).

proximal predentin toward the distal third [5, 6]. A reverse gradient is detected with 5D4, an antibody raised against KS (6). The increased KS labeling seen in the distal predentin near the mineralization front is confirmed by using an anti-lumican antibody, lumican being a KSPG [6–8]. Because MMP-3 (stromelysin-1) is visualized at the junction between the inner and central predentin [6], it is possible that the degradation of CS/DS facilitates the access of KS to the outer predentin where events preceding mineralization occur.

Using antibodies raised against BGN and DCN of rat incisors, we have previously shown that biglycan displayed an uniform distribution throughout predentin, whereas a threefold increase was detected for gold-anti-DCN conjugates in the distal predentin compared with the proximal and central parts [23]. The decorin increase near the mineralization front suggests a relationship between this SLRP and dentin mineralization. However, this result is conflicting with the decreasing gradient of CS/DS observed with the 2B6 antibody, as decorin is known to be a CS/DS PG. A possible explanation of the phenomenon is that decorin is deglycosylated during its transfer throughout predentin. Indeed, the protein core displays an increasing concentration toward the mineralization front, but a decrease in CS/DS chains as the glycan chains are degraded. In this context, immunolabeling for MMP-3, immunodetected as a band at the junction between the inner proximal and central predentin, provides data in favor of this hypothesis [6]. It is well documented that MMP-3 acts as a proteoglycanase [24, 25]. MMP-7 that induces cleavage sites at the N-terminal where the GAG chain is attached to the protein core might be an alternative candidate for promoting such an event, if indeed present in predentin [26]. Alternatively, it is also possible that DCN in predentin is directly synthesized as a protein and not as a proteoglycan, as in human skin [27].

Taken together, light and electron microscope immunostaining revealed a more complex organization of PGs in predentin than previously suspected. It established not only the occurrence of reverse gradients between CS/DS and KS, but also between CS/DS and decorin [3, 5, 6, 23].

Light Immunostaining of DCN, BGN and FM

The following new data were obtained with light microscopy immunostaining for DCN and BGN in newborn mouse. In day-1 mouse molars, the distribution was similar to that observed for the rat incisor, except that the DCN gradient reported above was less obvious. Table 1 shows that the immunostaining for each of the three SLRP antibodies was intense in predentin, strong in pre- and secretory ameloblasts, and also positive either at the junction between ameloblasts and the stratum intermedium, or in cells of the latter. It was weak, and roughly at background levels, in other areas.

Ultrastructural and Immunohistochemical Observations

Observations and measurements carried out in the wild-type mouse molar showed first, that the mean diameter of collagen fibrils was smaller than in the rat incisor, and second, that fibrillogenesis occurred mostly in the inner third of the predentin with the average fibril diameter remaining constant in the central and distal thirds. Interestingly, previous results have shown that the average diameter of the collagen fibrils in the rat incisor increased on a regular basis from the inner (20 nm) to the central (40 nm) and distal parts (55–75 nm) [13]. These differences in collagen fibrillogenesis between the mouse molar and the rat incisor are probably related to species differences but also could be related to the fact that one is a continuously erupting incisor and the other a molar of limited growth.

In the BGN KO, immunostaining for decorin and fibromodulin was about the same as in wild-type mice, whereas BGN staining was at a background level, confirming that BGN was not expressed in the dental tissues of the BGN KO mice.

Ultrastructural studies of the first molar at day 1 from a BGN KO revealed that odontoblasts displayed a normal appearance. Thin collagen fibrils and granules were observed in the inner part of predentin. A quantitative analysis of fibril diameters established that the average diameter of the collagen fibrils in the proximal third of the predentin was thinner in the BGN KO than in wild-type. In contrast, in the central and distal predentin, average fibril diameter was larger for the BGN KO than in the wild-type mice (Table 2). Similarly to what was observed in the wild-type, the average fibril diameter remained constant between the central and distal parts of the predentin in the BGN KO. The decorin core protein inhibits collagen fibrillogenesis, and fibrils formed in vitro in the presence of lumican and decorin are significantly thinner that fibrils formed in the absence of proteoglycan [28]. In contrast, fibromodulin-null mice have thinner fibrils in tail tendons than wild-type animals [29]. BGN is known to interact with type I collagen [30]. SLRPs are horseshoe-shaped molecules, help to stabilize collagen fibrils, and have been implicated in orienting fibrillogenesis [31]. The present data demonstrate that the absence of BGN alters the collagen fibrillogenesis in predentin.

Metadentin [20] was broadened and more porous in the BGN KO compared with the wild mouse (Figure 1). In circumpulpal dentin, small and larger nodules did not merge, and numerous interglobular spaces gave a porous appearance to the dentin. The mantle dentin, near the dentinoenamel junction, was also less mineralized than in the wild-type mouse, and appeared more heterogeneous. These alterations are reminiscent of the age-dependent osteopenia and an osteoporosis-like phenotype observed in the BGN KO [21]. Taken together, our data support the hypothesis that BGN plays an important role in the formation and mineralization of dentin.

ACKNOWLEDGMENTS

This work was supported by grants from the Wellcome Trust Fundation and by STSM from the Cost action B8 Odontogenesis. We thank Ake Oldberg and Shuki Chakravarti for providing the FM KO mice.

REFERENCES

[1] Linde, A., and Goldberg, M. (1993). Dentinogenesis. *Crit. Rev. Oral Biol. Med.* 4:679–728.

[2] Goldberg, M., and Takagi, M. (1993). Dentin proteoglycans: Composition, ultrastructure and functions. *Histochem. J.* 25:781–806.

[3] Embery, G., Hall, R., Waddington, R., Septier, D., and Goldberg, M. (2001). Proteoglycans in dentinogenesis. *Crit. Rev. Oral Biol. Med*. 12:331–349.

[4] Lormée, P., Septier, D., Lécolle, S., Baudouin, C., and Goldberg, M. (1996). Dual incorporation of (35S)sulfate into dentin proteoglycans acting as mineralization promotors in rat molars and predentin proteoglycans. *Calcif. Tiss. Int.* 58:368–375.

[5] Septier, D., Hall, R.D., Lloyd, D., Embery, G., and Goldberg, M. (1998). Quantitative immunohistochemical evidence of a functional gradient of chondroitin 4-sulphate/dermatan sulphate, developmentally regulated in the predentine of rat incisor. *Histochem. J.* 30:275–284.

[6] Hall, R., Septier, D., Embery, G., and Goldberg, M. (1999). Stromelysin-1 (MMP-3) in forming enamel and predentine in rat incisor—coordinated distribution with proteoglycans suggests a functional role. *Histochem. J.* 31:761–770.

[7] Iozzo, R.V. (1999). The biology of the small leucine-rich proteoglycans: Functional network of interactive proteins. *J. Biol. Chem.* 274:18843–18846.

[8] Neame, P.J., and Kay, C.J. (2000). Small Leucine-rich proteoglycans. In *Proteoglycans—Structure, Biology and Molecular Interactions*, R.V. Iozzo (ed.), pp. 201–235 (Marcel Dekker, New York).

[9] Buchaille, R., Couble, M.L., Magloire, H., and Bleicher, F. (2000). Expression of the small leucine-rich proteoglycan osteoadherin/osteomodulin in human dental pulp and developing rat teeth. *Bone* 27:265–270.

[10] Takagi, M., Hishikawa, H., Hosokawa, Y., Kagami, A., and Rahemtulla, F. (1990). Immunochemical localization of glycosaminoglycans and proteoglycans in predentin and dentin of rat incisors. *J. Histochem. Cytochem.* 38:319–324.

[11] Yoshiba, N., Yoshiba, K., Iwaku, M., and Ozawa, H. (1996). Immunolocalization of the small proteoglycan decorin in human teeth. *Arch. Oral Biol.* 41:351–357.

[12] Zhang, C.Z., Bartold, P.M., Young, W.G., and Waters, M.J. (1995). Effect of growth hormone on the distribution of decorin and biglycan during odontogenesis in the rat incisor. *J. Dent. Res*. 74:1636–1643.

[13] Goldberg, M., Septier, D., and Escaig-Haye, F. (1987). Glycoconjugates in dentinogenesis and dentine. *Progr. Histochem. Cytochem*. 17/2:1–113.

[14] Hunter, G.K. (1991). Role of proteoglycan in the provisional calcification of cartilage. A review and reinterpretation. *Clin. Orthopaed*. 262:256–280.

[15] Poole, A.R., Pidoux, I., and Rosenberg, L. (1982). Role of proteoglycans in endochondral ossification: Immunofluorescent localization of link protein and proteoglycan monomer in bovine epiphyseal growth plate. *J. Cell Biol*. 92:249–260.

[16] Chen, C.-C., and Boskey, A.L. (1985). Mechanisms of proteoglycan inhibition of hydroxyapatite growth. *Calcif. Tiss. Int.* 37:395–400.

[17] Linde, A., Lussi, A., and Crenshaw, M.A. (1989). Mineral induction by immobilized polyanionic proteins. *Calcif. Tiss. Int*. 44:286–295.

[18] Gafni, G., Septier, D., and Goldberg, M. (1999). Effect of chondroitin sulfate and biglycan on the crystallization of hydroxyapatite under physiological conditions. *J. Crystal Growth* 205:618–623.

[19] Fisher, L.W., Stubbs III, J.T., and Young, M.F. (1995). Antisera and cDNA probes to human and certain animal model bone matrix noncollagenous proteins. *Acta Orthop. Scand.* 66:61–65.

[20] Goldberg, M., and Septier, D. (1996). A comparative study of the transition between predentin and dentin, using various preparative procedures in the rat. *Eur. J. Oral Sci.* 104:269–277.

[21] Xu, T., Bianco, P., Fisher, L.W., Longenecker, G., Smith, E., Goldstein, S., Bonadio, J., Boskey, A., Heegaaard, A.-M., Sommer, B., Satomura, K., Dominguez, P., Zhno, C., Kulkarni, A.B., Gehron Robey, P., and Young, M.R. (1998). Targeted disruption of the biglycan gene leads to an osteoporosis-like phenotype in mice. *Nat. Genet.* 20:78–82.

[22] Chen, X.-D., Shi, S., Xu, T., Gehron-Robey, P., and Young, M. Age-related osteoporosis in biglycan deficient mice is related to defects in bone marrow stromal cells. *J. Bone Min. Res.*, in press.

[23] Septier, D., Hall, R.C., Embery, G., and Goldberg, M. (2001). Immunoelectron microscopic visualization of pro- and secreted forms of decorin and biglycan in the predentin and during dentin formation in the rat incisor. *Calcif. Tiss. Int.* 69:38–45.

[24] Birkedal-Hansen, H. (1995). Proteolytic remodeling of extracellular matrix. *Curr. Opin. Cell Biol.* 7:728–735.

[25] Bode, W., Fernandez-Catalan, C., Tschesche, H., Grams, F., Nagase, H., and Maskos, K. (1999). Structural properties of matrix metalloproteinases. *Cell Mol. Life Sci.* 55:639–652.

[26] Imai, K., Hiramatsu, A., Fukushima, D., Pierschbacher, M.D., and Okada, Y. (1997). Degradation of decorin by matrix metalloproteinases: Identification of the cleavage sites, kinetic analyses and transforming growth factor-β1 release. *Biochem. J.* 322:809–814.

[27] Fleischmajer, R., Fisher, L.W., macDonald, E.D., Jacob, L. Jr., Perlish, J.S., and Termine, J.D. Decorin interacts with fibrillar collagen of embryonic and adult human skin. *J. Struct. Biol.* 106:82–90.

[28] Rada, J., Cornuet, P.K., and Hassell, J.R. (1993). Regulation of corneal collagen fibrillogenesis in vitro by corneal proteoglycan (lumican and decorin) core proteins. *Exp. Eye Res.* 56:635–648.

[29] Svensson, L., Aszodi, A., Reinholt, F.P., Fassler, R., Heinegard, D., and Oldberg, A. (1999). Fibromodulin-null mice have abnormal collagen fibrils, tissue organization, and altered lumican deposition in tendon. *J. Biol. Chem*. 274:9636–9647.

[30] Schönherr, E., Witsch-Prehm, P., Harrach, B., Robeneck, H., Rauterberg, J., and Kresse, H. (1995). Interaction of biglycan with type I collagen. *J. Biol. Chem*. 270:2776–2783.

[31] Scott, J.E. (1996). Proteodermatan and proteokeratan sulfate (decorin, lumican/fibromodulin) proteins are horseshoe shaped. Implications for their interactions with collagen. *Biochemistry* 35:8795–8799.